Universal bond correlation function for two-dimensional polymer rings

Sakaue, Takahiro
Department of Physics, Kyushu University | PRESTO, Japan Science and Technology Agency

Witz, Guillaume
Laboratoire de Physique de la Matière Vivante, Ecole Polytechnique Fédérale de Lausanne

Dietler, G.
Laboratoire de Physique de la Matière Vivante, Ecole Polytechnique Fédérale de Lausanne

Wada, Hirofumi
Yukawa Institute for Theoretical Physics, Kyoto University

KYUSHU UNIVERSITY

epl draft

Universal bond correlation function for two-dimensional polymer rings

T. Sakaue[1,2] [(a)], G. Witz[3], G. Dietler[3] and H. Wada[4] [(b)]

[1] *Department of Physics, Kyushu University 33, Fukuoka 812-8581, Japan*
[2] *PRESTO, Japan Science and Technology Agency (JST), 4-1-8 Honcho Kawaguchi, Saitama 332-0012, Japan*
[3] *Laboratoire de Physique de la Matière Vivante, Ecole Polytechnique Fédérale de Lausanne (EPFL), CH-1015 Lausanne, Switzerland*
[4] *Yukawa Institute for Theoretical Physics, Kyoto University, Kyoto 606-8502, Japan*

Abstract. - The bond orientational correlation function (BCF) of a semiflexible ring polymer on a flat surface is studied theoretically. For a stiff chain, we give an exact analytic form of BCF with perturbation calculations. For a chain sufficiently longer than its persistence length, the conventional exponential decay vanishes and a long-range order along the chain contour appears. We demonstrate that the bond orientational correlation satisfies the scaling properties, and construct an interpolating formula for its universal curve that encompasses the short- and large-distance behaviors. Our analytical findings are confirmed by extensive Langevin dynamics simulations, and are in excellent agreement with recent experimental data obtained from DNA molecules imaged by atomic force microscopy without any fitting parameters.

Introduction. – Circular polymers represent an important class of macromolecules not only found in living organisms, but also employed in modern biotechnology. The interplay between topology, mechanical and entropic elasticities determines the equilibrium shape of DNA minicircles and larger plasmids [1,2]. For the targeted search by proteins along genomic DNA [3,4], long range spatial and temporal interactions arising from such interplay are known to be crucial. While physical properties of circular polymers are significantly different from those of linear polymers, an understanding comparable to that of open polymers is still lacking [5–14]. A central complication lies in the topological constraint that severely restricts a rigorous theoretical treatment. Here we tackle this problem by studying the bond orientational correlation function (BCF) of a semiflexible ring polymer on a flat surface by combining analytical and numerical approaches.

Polymers are one-dimensional curves embedded in higher space dimensions, and the bond orientational correlation function (BCF) is a basic quantity characterizing their conformation. One may often assume its exponential decay, which then leads to the quantification of the persistence length, a fundamental length scale in a polymer chain. In many realistic situations, the BCF exhibits more interesting and complicated features, and its physical interpretation should be carefully made. Several studies have considered particular cases of polymers such as in melts [15], at the Θ-point [16,17] or with short range repulsion [18], but these studies so far seem mostly devoted to linear chain systems, and do not help resolve recent experimental data on circular DNA [19,20].

Scaling concepts have been successfully applied to various problems in polymer physics for years [21,22]. A complete physical picture of planar polymer ring conformations is however still lacking, making it unclear whether a scaling argument is sufficient to understand global-topology-preserving polymer chains. This concern directly links to a key issue on whether or not global topological effects can be mapped into fictitious local interactions. In this paper, we provide (to our knowledge) the first successful example of such a mapping by demonstrating a quantitative agreement between a scaling approach and the corresponding experiments and numerical simulations. We

[(a)]E-mail: `sakaue@phys.kyushu-u.ac.jp`
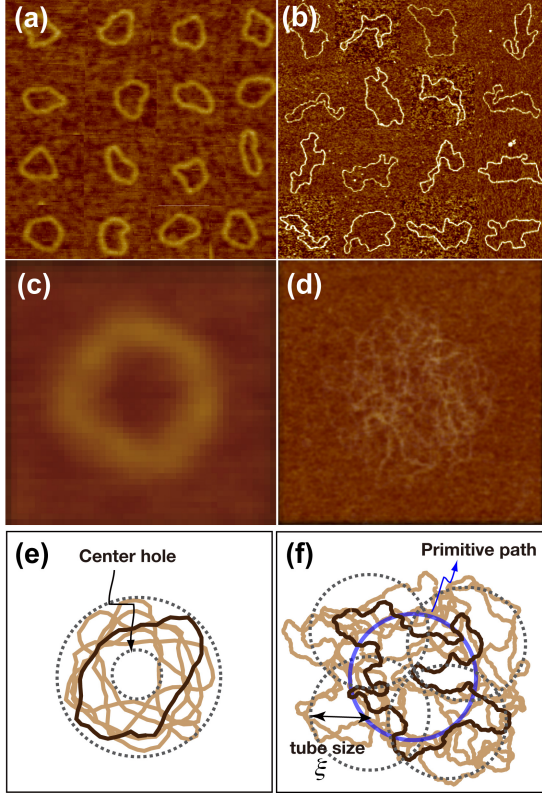[(b)]E-mail: `hwada@yukawa.kyoto-u.ac.jp`

Fig. 1: Images of DNA plasmids and simulation snapshots. (a) DNA mini-circles ($L \simeq 230$ nm). (b) pSH1 plasmids ($L \simeq 2016$ nm). (c) and (d) Superposition in the center-of-mass frame of pictures of (a) and (b), respectively. (e) and (f) Superposition in the center-of-mass frame of chain configurations from our simulations for $\chi \simeq 7$, and $\chi \simeq 110$. In black, representative snapshot taken at random.

investigate the functional form of BCF of a circular chain confined in two-dimensions over the entire range of flexibility $\chi \equiv L/\ell_p$, where L and ℓ_p are the contour length and the persistence length of the chain. For $\chi \ll 1$, where a ring takes a nearly circular shape with small fluctuations around it, the exact analytic expression of the BCF is obtained within a Gaussian theory. For $\chi \gg 1$, measurements of the average monomer distribution indicates that the equilibrium chain configuration is adjusted so that it just closes the central hole region. This essential observation leads us to the *self-confinement* picture, through which we introduce a concept of "topological blob" characterizing the spatial size of the confinement. By combining the Gaussian theory and the scaling arguments, we construct an interpolating formula for BCF that encompasses the short- and large-distance behaviors. Our analytical findings are confirmed by extensive Langevin dynamics (LD) simulations, and are in excellent agreement with our experimental data obtained from DNA molecules imaged by atomic force microscopy (AFM). In the present paper, we propose a generic idea on how to map global topological effects such as circularity into fictitious local interactions

of open polymers, which may help inspire a further development of the understanding on topologically constrained polymers.

Numerical simulation methods. – Before describing our analytical approaches, we briefly mention our simulation details. In our LD simulations, a polymer is modeled as a chain of M connected spheres of diameter a confined in the two-dimensional space. The total potential energy includes three contributions $U = U_{str} + U_{LJ} + U_{bend}$. The stretching energy

$$U_{str} = \frac{K}{2} \sum_{i=1}^{M-1} (|\mathbf{r}_{i+1} - \mathbf{r}_i| - a)^2 \qquad (1)$$

ensures the connectivity of spheres, where $\mathbf{r}_i$ is the two-dimensional position vector of sphere i. We take the modulus K large enough to make the bond length fluctuations negligible. The truncated Lennard-Jones (LJ) potential,

$$U_{LJ} = \epsilon_{LJ} \sum_{i<j} \left(\frac{a^6}{|\mathbf{r}_i - \mathbf{r}_j|^6} - \frac{a^{12}}{2|\mathbf{r}_i - \mathbf{r}_j|^{12}} \right), \quad (2)$$

makes the ring non-ideal, and at the same time prevents chain self-crossings in order to fix the ring topology. We take $\epsilon_{LJ} = k_B T$, where $k_B T$ is the thermal energy. The bending energy

$$U_{bend} = \frac{k_B T \ell_p}{a} \sum_{i=1}^{M} \left(1 - \frac{\mathbf{u}_{i-1} \cdot \mathbf{u}_i}{a^2} \right), \qquad (3)$$

accounts for the stiffness of the chain backbone, where $\mathbf{u}_i = \mathbf{r}_{i+1} - \mathbf{r}_i$ is the bond vector. The dynamics of the chain follows the Langevin equation

$$m \frac{d^2 \mathbf{r}_i}{dt^2} = -\gamma \frac{d \mathbf{r}_i}{dt} - \nabla_{\mathbf{r}_i} U + \boldsymbol{\xi}_i(t), \qquad (4)$$

where m and γ are the mass and friction coefficient of a monomer, and the random force vector $\boldsymbol{\xi}$ satisfies the fluctuation-dissipation relations

$$\langle \boldsymbol{\xi}_i(t) \boldsymbol{\xi}_j(t') \rangle = 2\gamma k_B T \mathbf{1} \delta_{ij} \delta(t - t'). \qquad (5)$$

where $\mathbf{1}$ is a 2×2 unit matrix. Since we are only interested in the equilibrated conformations of the chain, solvent-mediated hydrodynamic interactions between distant monomers are totally ignored. We discretize our Langevin equations with the time step Δt, and perform numerical integration using a leapfrog algorithm. We rescale all quantities by the sphere diameter a, the thermal energy $k_B T$, and the unit time $\tau = \gamma a^2 /(k_B T)$. For sufficient numerical accuracy, we adopt the time step $\Delta t/\tau = 0.005$. Total simulation times are up to 10^9 steps, and data are averaged over several independent runs for sufficient statistics. To highlight the topological effect, a comparative analysis for freely self-crossing rings is also performed by setting $\epsilon_{LJ} = 0$. We refer to the model with and without U_{LJ} as, respectively, a self-avoiding ring (SAR) and an ideal phantom ring (IPR).

Stiff chains: Gaussian perturbation theory. – To proceed, we first present the Gaussian theory of a stiff circle whose contour length is smaller or comparable to its persistence length. A closed curve is parameterized by the arc-length $s \in [0, L]$, whose unit tangent vector at s is given by $\mathbf{t}(s) = (-\sin\theta(s), \cos\theta(s))$. For a perfect circle, we have $\theta(s) = \theta_0(s) = 2\pi s/L$. The bending energy of the ring is described by

$$E \;=\; \frac{k_B T \ell_p}{2} \int_0^L (\partial_s \mathbf{t})^2 ds, \qquad (6)$$

where ∂_s represents the derivative with respect to s. The torsional elasticity of the ring is neglected in this study, as valid for nicked DNA rings used in the experiments [19]. Expanding E in terms of small fluctuations $\delta\theta(s) = \theta - \theta_0$, and writing $\delta\theta(s)$ as the discrete Fourier series:

$$\delta\theta(s) \;=\; \frac{1}{L} \sum_{n=-\infty}^{\infty}{}' \tilde{\theta}_n e^{2\pi i n s/L}, \qquad (7)$$

we obtain

$$E \;=\; \frac{4\pi^2 k_B T \ell_p}{L^3} \sum_{n=2}^{\infty} n^2 |\tilde{\theta}_n|^2. \qquad (8)$$

Note that the prime in summation in eq. (7) implies to exclude the modes $n = \pm 1$, as well as $n = 0$, to ensure the closure condition: $\int_0^L \delta\mathbf{t}(s)ds = 0$ [23]. Applying equipartition, we obtain

$$\langle |\tilde{\theta}_n|^2 \rangle \;=\; \frac{L^3}{4\pi^2 \ell_p n^2} \qquad (9)$$

for $n \geq 2$. The bond correlation function is defined as

$$G(s) = \langle \mathbf{t}(s) \cdot \mathbf{t}(0) \rangle = \langle \cos[\theta(s) - \theta(0)] \rangle. \qquad (10)$$

The ring architecture assures the translational invariance $\langle \mathbf{t}(s_1) \cdot \mathbf{t}(s_2) \rangle = \langle \mathbf{t}(s) \cdot \mathbf{t}(0) \rangle$ for $s = |s_1 - s_2|$ and the inversion symmetry $G(s) = G(L - s)$. Expanding eq. (10) in powers of $\delta\theta$ up to the quadratic order, and using eq. (9), we obtain

$$G(s) = \left[1 + \frac{L}{2\pi^2 \ell_p} \left\{ g\left(\frac{2\pi s}{L}\right) - g(0) \right\} \right] \cos\left(\frac{2\pi s}{L}\right). \qquad (11)$$

where

$$g(z) \;=\; \sum_{n=2}^{\infty} \frac{\cos(nz)}{n^2} = \frac{(\pi - z)^2}{4} - \frac{\pi^2}{12} - \cos z. \quad (12)$$

In fig. 2 (left), eq. (11) is compared to the numerical data obtained from our LD simulations for two different models, *i.e.*, a self-avoiding ring chain (SAR) and an ideal phantom ring chain (IPR). Remarkably, the agreement is excellent even for $\chi \simeq 6$. Approaching the stiff limit $G(s) \to \cos(2\pi s/L)$ with $\chi \to 0$, the negative curvature
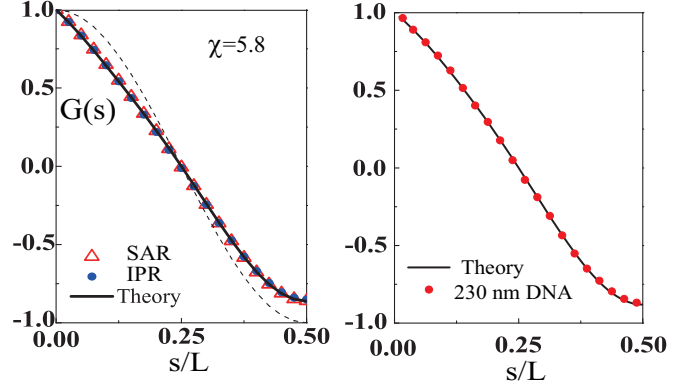

Fig. 2: (Left) Bond correlation function (BCF) for $\chi \simeq 5.8$ as a function of the rescaled contour length s/L. Data points are obtained from our LD simulations, and the solid line is eq. (11). The dotted curve represents the BCF for a circle, $\cos(2\pi s/L)$. (Right) Fit of eq. (11) to the experimental BCF obtained from 230 nm long DNA [19].

in the initial part of $G(s)$ develops. Indeed, the condition $\partial_s^2 G(s)|_{s=0} < 0$ could be a practical sign of the stiff regime. From this criterion, we numerically determine the crossover point as $\chi_* = 8$, below which a polymer is regarded to be in the stiff regime and no self-crossing of the chain is expected. This makes the data from SAR and IPR undistinguishable, as seen in fig. 2 (left). It is helpful to keep in mind, what this crossover means in terms of the conformation of the polymer. For stiff rings, there is a center region enclosed by the polymer, where no monomers are found, see fig. 1 (c) or (e). Increasing the flexibility leads to a progressive narrowing of the center hole. The hole eventually disappears at the limit χ_*, which implies interactions between distant parts of the ring, compare fig. 1 (c) and (d). As a consequence, the breakdown of the Gaussian approximation signals the onset of the interplay between excluded volume effects and topology, which are essential in the flexible regime.

The analytical formula, eq. (11) is also successfully applied to the experimental data of two-dimensional equilibrated circular DNA imaged by AFM (for experimental details see [19]). We give an example in fig. 2 (right), where we fit eq. (11) to the data by treating the persistence length ℓ_p as a fitting parameter. The obtained value of $\ell_p = 45$ nm, i.e. $\chi \simeq 5$ for this polymer, is in good agreement to the values for longer chains (49-52 nm) obtained previously from the initial exponential decay in their BCF [19], given the different theories used in the two studies. In particular, eq. (11) provides a way to measure directly the persistence length of short rigid circular molecules that was not available previously [19].

Flexible chains: scaling regimes. – For the flexible regime, we compare now in fig. 3 the BCFs of IPRs and SARs obtained from our numerical simulations. Clearly, self-avoidance has a dramatic effect in this regime. To unveil the scaling structure in the BCF, let us begin with the
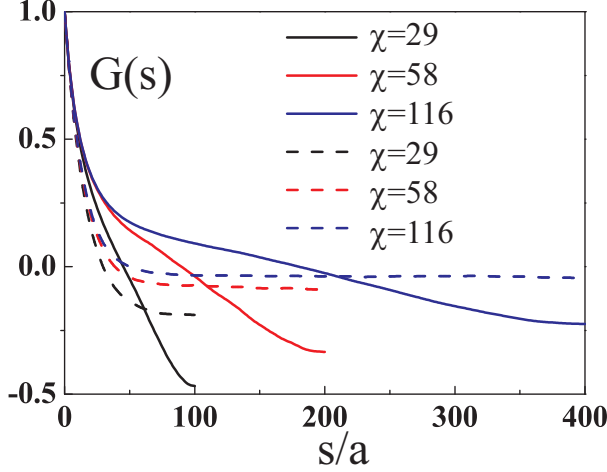
Fig. 3: Bond correlation functions for SARs (solid curves) and IPRs (dashed curves) obtained from our LD simulations for various values of χ, as a function of the (dimensionless) contour length s/a, where a is the monomer diameter.

Fig. 4: (Left) Scaling plot of the BCF, $\phi(s/L)$, obtained from our simulations of SARs for different χ. (Right) $\phi(s/L)$ obtained from 2000 nm-long circular DNA [19]. In both figures, the analytic formula eq. (18) is also plotted.

trivial example of IPRs. The only sources of correlation are the bending rigidity and the sum rule $\int_0^L ds G(s) = 0$ which is a consequence of circularity [24]. The first item leads to an initial exponential decay with $G(s) \sim e^{-s/2\ell_p}$, and the second item can be rewritten as $\int_{2\ell_p}^L ds G(s) \simeq -1$. The absence of any long-range interactions in IPRs results in the equipartitioning of the returning correlation at a constant weak negative level, $G(s) \sim -\ell_p/L$ for $s \gg 2\ell_p$. This disappears in the long chain limit, i.e., $G(s) = 0$ for $L/\ell_p = \infty$ [24].

The above considerations suggest that $G(s, L)$ for IPRs of different chain lengths can be collapsed onto a single master curve, $\phi(s/L) = (\ell_p/L)^{-1} G(s, L)(\simeq -1)$. Indeed, the presence of such a scaling,

$$\phi(s/L) = \left(\frac{\ell_p}{L}\right)^\alpha G(s, L), \qquad (13)$$

is not accidental in this simple example only, but rather a general consequence of the self-similar structure of the flexible chains. One can elaborate its scaling structure by making use of the relation [15, 18]

$$G(s - s') = \langle \partial_s \mathbf{r} \cdot \partial_{s'} \mathbf{r} \rangle = -\frac{1}{2} \partial_s \partial_{s'} \langle R^2(s - s') \rangle, \quad (14)$$

where $\langle R^2(s - s') \rangle$ is the internal end-to-end distance. For IPRs, $\langle R^2(s) \rangle \simeq \ell_p s (1 - s/L)$ where a correction term $-s/L$ appears due to the circularity [25]. Since the leading term vanishes after the second derivative, this small term is responsible for the formula $\alpha = -1$ and $\phi(x) \simeq -1$ given above. For linear chains with excluded volume interactions (characterized by the non-ideal exponent $\nu = 3/4$ in two dimensions), this indicates a power-law decay in the bond correlation $\phi(x) = x^{-1/2}$ with $\alpha = 2\nu - 2 = -1/2$. For SARs, the rigorous relation for the internal end-to-end distance is not available. Nevertheless, our physical picture
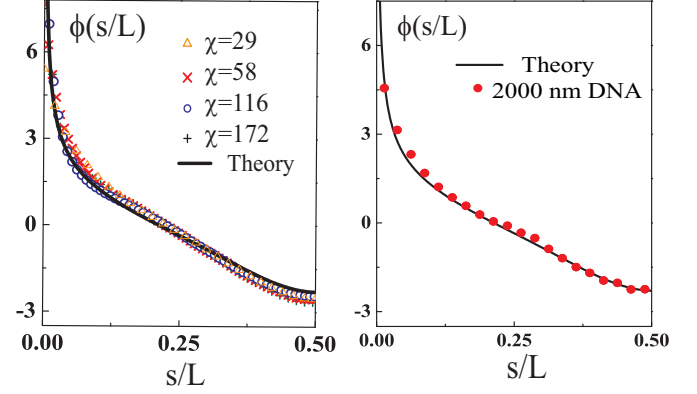
described below suggests $\phi(s/L) = (\ell_p/L)^{-1/2} G(s, L)$, indicating that all the circularity effects are absorbed into the functional form of $\phi(s/L)$ while α is solely determined by the swelling exponent ν. We numerically verified that this scaling ansatz, first proposed by Baumgärtner [26] in a different model (i.e., a ring with no topological constraint), works perfectly (fig. 4 (left)).

Interpolating formula. – Our final task is to deduce the universal scaling function $\phi(x)$ for SARs. To see the importance of the topology, we tentatively adopt an approximation formula for the internal end-to-end distance proposed by Bloomfield and Zimm [27]:

$$\langle R^2(s) \rangle = c \, \ell_p^{2-2\nu} \frac{s^{2\nu}(L-s)^{2\nu}}{s^{2\nu} + (L-s)^{2\nu}}, \qquad (15)$$

which accounts (i) for the inversion symmetry $\langle R^2(s) \rangle = \langle R^2(L-s) \rangle$ due to circularity and (ii) for the non-ideality due to the excluded volume effect through the exponent ν. In spite of its simple construction, it provides a fairly good description for $\langle R^2(s) \rangle$. The factor $c = 1.56$ in eq. (15) was fixed from numerical simulation for our two-dimensional ring. Surprisingly, however, the scaling form of the BCF obtained from eq. (14) and (15)

$$\phi_S(y) = \frac{c}{2} \frac{\partial^2}{\partial y^2} \left[\frac{y^{2\nu}(1-y)^{2\nu}}{y^{2\nu} + (1-y)^{2\nu}} \right]. \qquad (16)$$

works well only at a small separation $s/L \lesssim 0.1$. Unlike for a linear chain, the power-law decay of BCF disappears at around $s/L \simeq 0.1$ and the curve shows a *negative* curvature in the middle range before taking zero at $s/L \simeq 0.23$ (see fig. 4). The reason for this disagreement is that the interplay of topology and excluded volume interactions is missing in eq. (15), and this becomes evident only when taking the second derivative of eq. (15).

To handle this self-interaction of topological origin, one can replace the global constraint by a fictitious tube and

envision the chain to be *confined* within it [6]. The average path of length $\mathcal{L}$ depicted in fig. 1 (f) is the analogue of the primitive path used in the reptation theory [28]. The particular feature of our system is that the tube is configured by the molecule itself, and encloses *topological blobs* of radius ξ. According to the analogy with a polymer confined in a tube, the length scale ξ is set in such a way that each part of the ring just comes into unavoidable contact with others. In a coarse-grained frame, the primitive chain acquires an effective bending elasticity arising from excluded volume interactions among topological blobs. These topological blobs cover the internal area of the ring in such a way that there exists no center hole, and the blob size ξ represents an effective persistence length. Recalling the physical meaning of the crossover point χ_*, the above statement is expressed as $\chi_* \sim \mathcal{L}/\xi$, i.e., the primitive chain actually resides on the crossover point, no matter how long the chain is. More compact configurations would need a larger pressure, while more extended ones would result in entropy loss; both are thermodynamically unfavorable. This ensures the use of the Gaussian approximation to analyze the primitive path fluctuations. With this conceptual renormalization, the chain contour length L and the persistence length ℓ_p appearing in eq. (11) should be replaced with the contour length of the primitive path $\mathcal{L}$ and the blob size ξ.

The BCF of the primitive path, whose arc length is parameterized by $0 < \sigma < \mathcal{L}$, is given by eq. (11), with the substitutions of $L/\ell_p \to \chi_*$ and $s/L \to \sigma/\mathcal{L}$. The obtained function is re-interpreted as that of the true chain. The scaling function in this regime is therefore given by

$$\phi_L(y) = \chi_*^{1/2} \left[1 + \frac{\chi_*}{2\pi^2} \left\{ g(2\pi y) - g(0) \right\} \right] \cos(2\pi y), \quad (17)$$

where a possibility of order-of-one prefactor was omitted, which is justified later on from the comparison to the experimental data.

Having clarified the physical pictures of chain's short- and long- distance behaviors, we now construct a formula for the bond correlation. Within a topological blob of size ξ, the chain is a self-avoiding walk free from the topological constraint and its BCF is given by eq. (16). At length scale larger than ξ, however, the fine-grained structure becomes irrelevant, and the global topological effect controls the BCF, see eq. (17). We propose a linear interpolation for the scaling function,

$$\phi(y) = 2y\phi_L(y) + (1 - 2y)\phi_S(y), \quad (18)$$

which encompasses the short scale behavior, eq. (16), and the large scale limit, eq. (17). This simple interpolation formula describes the simulation data perfectly over the entire available length range in fig. 4 (left). Agreement with the AFM experimental data in fig. 4 (right) is also remarkable. In both cases, there is no fitting parameter, meaning that the analytical, numerical, and experimental results all collapse onto the single master curve.

For completeness, we note that there is an additional regime at the shortest scale $s < \ell_p$, where the conformation is almost a rod-like. This finite size effect indicates a lower limit for the applicability of formula (18) at $s_\natural \simeq \ell_p \Leftrightarrow (s/L)_\natural = c_0\chi^{-1}$, below which the bending elasticity dominates. The numerical factor is estimated to be $c_0 = 4$ from the simulation data. A close inspection of Fig. 4 (left) shows this general trend in the small s/L region. One may appreciate its apparent effect for shorter/stiffer rings, for example, judged by a criteria $(s/L)_\natural > 0.25 \Leftrightarrow \chi < 16$. Finally, looking for the condition $(s/L)_\natural = 0.5$, i.e., the bending effect dominates the whole ring, we again find the crossover point $\chi_* = 8$.

Summary. – We have shown how the statistical behavior of semi-flexible rings can be separated into two regions: a first one, at small χ, dominated by mechanical constraints, and the other one, at large χ, dominated by topological and self-avoiding effects. We derived a formula allowing us to measure the rigidity of short rings and proved its applicability to DNA . We further unraveled the complex but *universal* behavior at large χ based on the self-confinement concept. This work offers a conceptual frame that could be eventually extended to other polymer properties. Among others, a generalization to three-dimensional case is an interesting but nontrivial issue where direct biological applications are possible. Work in this direction is now under progress.

$$* * *$$

REFERENCES

[1] Norouzi D., Mohammad-Rafiee F. and Golestanian R. , *Phys. Rev. Lett.*, **101** (2008) 168103.
[2] Demurtas D., *et al.*, *Nucleic Acids Res.*, **37** (2009) 2882.
[3] Halford S. E. and Marko J. F., *Nucleic Acids Res.*, **32** (2004) 3040.
[4] Gowers D. M. and Halford S. E., *EMBO J.*, **22** (2003) 1410.
[5] Descloizeaux J., *J. Phys. Lett.*, **42** (1981) L433.
[6] Grosberg A. Y., *Phys. Rev. Lett.*, **85** (2000) 3858.
[7] Deutsch J. M., *Phys. Rev. E*, **59** (1999) R2539.
[8] Dobay A., Dubochet J., Millett K., Sottas P. E. and Stasiak A., *Proc. Nat. Acad. Sci. U.S.A.*, **100** (2003) 5611.
[9] Deguchi T., and Tsurusaki K., *Phys. Rev. E*, **55** (1997) 6245.
[10] Araki S., Nakai T., Hizume K., Takeyasu K. and Yoshikawa K., *Chem. Phys. Lett.*, **418** (2006) 255.
[11] Alim K. and Frey E., *Eur. Phys. J. E*, **24** (2007) 185.

[12] ALIM K. and FREY E., *Phys. Rev. Lett.*, **99** (2007) 198102.

[13] DRUBE F., ALIM K., WITZ G., DIETLER G. and FREY E., *Nano Lett.*, **10** (2010) 1445.

[14] CAMACHO C. J., FISHER M. E. and SINGH R. R. P., *J. Chem. Phys.*, **94** (1991) 5693.

[15] WITTMER J. P.ET AL., *Phys. Rev. Lett.*, **93** (2004) 147801.

[16] SHIRVANYANTS D., PANYUKOV S., LIAO Q. and RUBINSTEIN M., *Macromolecules*, **41** (2008) 1475-1485.

[17] SHIMOMURA K., NAKANISHI H. and MITARAI N., *Phys. Rev. E*, **80** (2009) 051804.

[18] SCHÄFER L. and ELSNER K., *Eur. Phys. J. E*, **13** (2004) 225-237.

[19] WITZ G., RECHENDORFF K., ADAMCIK, J. and DIETLER G., *Phys. Rev. Lett.*, **101** (2008) 148103.

[20] RECHENDORFF K., WITZ G., ADAMCIK J. and DIETLER G., *J. Chem. Phys.*, **131** (2009) 095103.

[21] DE GENNES P. G., *Scaling concepts in polymer physics* (Cornell Univ. Press, Ithaca NY) 1979

[22] NETZ R. R. and ANDELMAN D., *Phys. Rep.*, **380** (2003) 1-95.

[23] PANYUKOV S. and RABIN Y., *Phys. Rev. E*, **62** (2000) 7135-7146.

[24] CROXTON C. A., *J. Phys. A: Math. Gen.*, **18** (1985) 995.

[25] ZIMM B. H. and STOCKMAYER W. H., *J. Chem. Phys.*, **17** (1949) 1301.

[26] BAUMGÄRTNER A., *J. Chem. Phys.*, **76** (1982) 4275.

[27] BLOOMFIELD. V and ZIMM B. H., *J. Chem. Phys.*, **44** (1966) 315.

[28] DOI M. and EDWARDS S. F., *The theory of polymer dynamics* (Clarendon Press, Oxford) 1986.